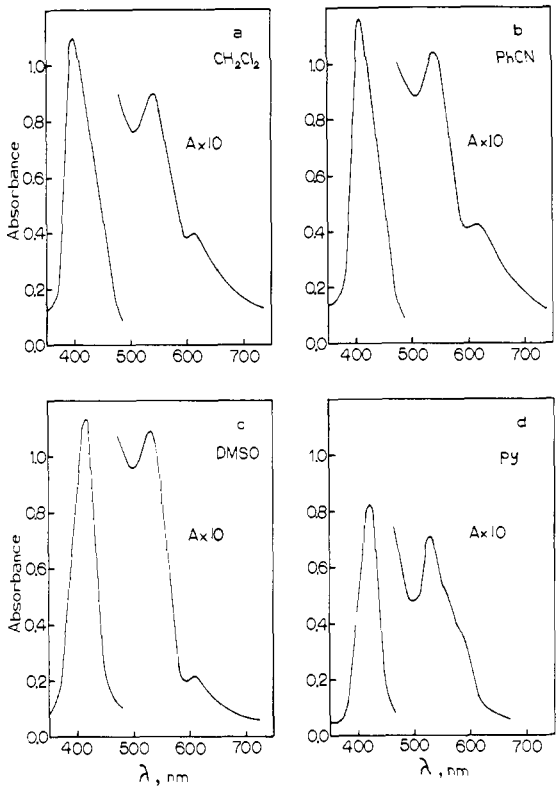

Figure 11. Electronic absorption spectra of (TPP)Fe(NO) in various solvents containing 0.1 M TBAP: (a) CH_2Cl_2, (b) PhCN, (c) Me_2SO, (d) py.

remain almost invariant in the nondissociating solvents of classes I and II. Also, it is of interest to note from Tables II and III that a larger solvent effect is noted for (TPP)Fe(NO)(S) than for (OEP)Fe(NO)(S).

Potentials for the first reduction of (TPP)Fe(NO) and (OEP)Fe(NO) can be compared to the potentials for (TPP)Fe and (OEP)Fe reduction in a number of solvents. An earlier study of solvent effects on the redox reactions of (TPP)Fe(S) and (TPP)Fe(S)$_2$ showed that $E_{1/2}$ (when corrected for liquid junction potential) was virtually independent of solvent.[14] This is not the case for (TPP)Fe(NO)(S) and (OEP)Fe(NO)(S). Binding of a solvent molecule results in an anodic shift of potential from that of (TPP)Fe(NO) or (OEP)Fe(NO) with the magnitude of the shift being dependent upon the solvent DN. The maximum potential difference of this shift is 150 mV between (TPP)Fe(NO) and (TPP)Fe(NO)(S) (where S = DMA or Me_2SO). A similar anodic shift is also observed for (OEP)Fe(NO)(S), but in this case the anodic shift was smaller in magnitude.

In conclusion, we have shown that the binding of one or two nitrosyl ligands to (TPP)Fe and (OEP)Fe generate dramatic shifts of redox potentials for oxidation and reduction of the stable Fe(II) complexes. For the case of (TPP)Fe(NO), the magnitude of shift in the Fe(III)/Fe(II) reaction with respect to (TPP)FeCl is approximately 1.0 V, independent of solvent. Similar values of $\Delta E_{1/2}$ are also observed between (OEP)Fe(NO) and (OEP)FeCl, but an even greater potential shift is observed after formation of (OEP)Fe(NO)$_2$, which is oxidized at a potential 200 mV anodic of (OEP)Fe(NO). These shifts of potential are comparable to those induced by the binding of CO to Fe(II),[1,39] but with NO as an axial ligand, stable oxidized complexes may be obtained. This is not true with CO, which does not bind to Fe(III). In this paper we have also spectrally identified the first reduced complex of Fe(II) with a bound axial ligand, $[PorFe(NO)]^{-1}$. Similar spectral identifications have been obtained for $[PorFe(NO)]^+$ and $[PorFe(NO)_2]^+$. These spectral and electrochemical characterizations of model Fe(II) complexes that have been oxidized or reduced are of importance in understanding the redox reactions of heme proteins with small diatomic molecules such as NO, CO, or O_2.

Acknowledgment. We are grateful for the financial support of this work from the National Institutes of Health (Grant GM 25172). We also with to thank Dr. S. Kelly for helpful discussions and R. Wilkins for making speciality electrochemical cells.

Registry No. (TPP)Fe(NO), 52674-29-0; (OEP)Fe(NO), 55917-58-3; (TPP)Fe(NO)$_2$, 53637-75-5; (OEP)Fe(NO)$_2$, 68879-28-7.

(39) Buchler, W. J.; Kokisch, W.; Smith, P. D. *Struct. Bonding (Berlin)* **1978**, *34*, 79.

Reduction Potentials for 2,2′-Bipyridine and 1,10-Phenanthroline Couples in Aqueous Solutions

C. V. Krishnan, Carol Creutz,* Harold A. Schwarz, and Norman Sutin

Contribution from the Department of Chemistry, Brookhaven National Laboratory, Upton, New York 11973. *Received February 7, 1983*

Abstract: From pulse-radiolysis studies of 2,2′-bipyridine (bpy), 1,10-phenanthroline (phen), and 4,4′-dimethyl-2,2′-bipyridine ($(CH_3)_2$bpy) and an analysis of the pH and free-energy dependence of the rate constants for quenching of poly(pyridine)-ruthenium(II) excited states by the above aromatic amines (L) and their protonated counterparts (LH^+, LH_2^{2+}), the following parameters concerning L and its one-electron reduction product $L^{-\cdot}$ have been deduced at 25 °C: for L = bpy, $pK_a(LH_2^{2+}) = 0.05$, $pK_a(LH^+) = 4.4$, $pK_a(LH_2^{+\cdot}) = 8.0$, $pK_a(LH^\cdot) \simeq 24$, $E°(LH_2^{2+}-LH_2^{+\cdot}) = -0.50$ V, $E°(LH^+-LH^\cdot) = -0.97$ V; for L = phen, $pK_a(LH_2^{2+}) = -0.2$, $pK_a(LH^+) = 4.9$, $pK_a(LH^\cdot) \simeq 24$, $E°(LH_2^{2+}-LH_2^{+\cdot}) = -0.47$ V, $E°(LH^+-LH^\cdot) = -0.85$ V; and for L = $(CH_3)_2$bpy, $pK_a(LH_2^{2+}) = 0.68$, $pK_a(LH_2^{+\cdot}) = 9.3$, $pK_a(LH^\cdot) \simeq 25$, $E°(LH_2^{2+}-LH_2^{+\cdot}) = -0.54$ V, $E°(LH^+-LH^\cdot) = -1.05$ V. The reduction potentials and other electron-transfer parameters of these and related couples are discussed.

The one-electron reduction of 2,2′-bipyridine (bpy) to $bpy^{-\cdot}$ is electrochemically reversible ($E_{1/2} = -2.13$ V vs. aqueous SCE) in acetonitrile[1] and *N*,*N*-dimethylformamide,[2] and the two-electron reduction process has been characterized in aqueous media.[3-5] Polarographic data have been reported for the one-electron process in water,[6] but the interpretation of these data is complicated by

(1) Tokel-Takvoryan, N. E.; Hemingway, R. E.; Bard, A. J. *J. Am. Chem. Soc.* **1973**, *95*, 6582.
(2) Saji, T.; Aoyagui, S. *J. Electroanal. Chem.* **1975**, *63*, 31.
(3) Erhard, H.; Jaenicke, W. *J. Electroanal. Chem.* **1975**, *65*, 675.
(4) Erhard, H.; Jaenicke, W. *J. Electroanal. Chem.* **1977**, *81*, 79.
(5) Erhard, H.; Jaenicke, W. *J. Electroanal. Chem.* **1977**, *81*, 89.
(6) Gurtler, O.; Dietz, K. P.; Thomas, P. *Z. Anorg. Allg. Chem.* **1973**, *398*, 217.

0002-7863/83/1505-5617$01.50/0

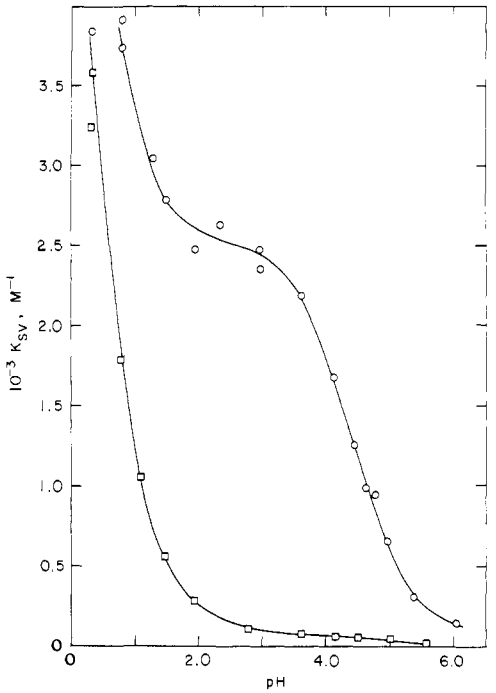

Figure 1. Stern–Volmer constant for quenching of $*Ru(4,7\text{-}(CH_3)_2phen)_3^{2+}$ (circles, $\tau_0 = 1.74 \times 10^{-6}$ s) and $*Ru(5,6\text{-}(CH_3)_2phen)_3^{2+}$ (squares, $\tau_0 = 1.81 \times 10^{-6}$ s) emission by 2,2′-bipyridine as a function of pH in 0.5 M ionic strength sulfate–bisulfate media.

the fact that the one-electron reduction product bpyH· (or $bpyH_2^{+}$· depending upon the pH) undergoes a rapid disproportionation reaction.[7] Equations 1 and 2 describe the sequence in basic solution. This disproportionation (and the low reduction potentials

$$bpy + e^- \xrightarrow{+H^+} bpyH\cdot \quad (1)$$

$$2bpyH\cdot \rightarrow bpyH_2 + bpy \quad (2)$$

of the one-electron couples) renders direct measurement of the reduction potentials of the $bpyH^+$–bpyH· and related couples very difficult in aqueous media. An understanding of these thermodynamics is, however, important in water photoreduction systems in which bpy is a component[8,9] since bpy reduction can occur at the expense of H_2O reduction. Here we have used the pulse-radiolysis technique and the well-characterized RuL_3^{3+}–$*RuL_3^{2+}$ couples[10-13] (L is a 2,2′-bipyridine or 1,10-phenanthroline derivative, $*RuL_3^{2+}$ denotes the luminescent excited state of RuL_3^{2+}) to estimate the reduction potential and self-exchange rate of the $bpyH^+$–bpyH· couple. The latter, taken with pK_a data we have determined and literature $E°$ data, have in turn been used to estimate the $E°$ values for the $bpyH_2^{2+}$–$bpyH_2^{+}$· and $bpyH^+$–bpyH· couples. In addition, data pertinent to the related 4,4′-dimethyl-2,2′-bipyridine ($(CH_3)_2bpy$) and 1,10-phenantholine (phen) systems are also reported.

Experimental Section

The RuL_3^{2+} samples were prepared as in ref 10; 2,2′-bipyridine and 1,10-phenanthroline were obtained from Fischer and 4,4′-dimethyl-2,2′-bipyridine from G. F. Smith. Stern–Volmer constants ($K_{SV} = [(I_0/I) - 1]/[Q]$) were obtained from emission intensity (I) data[10] determined

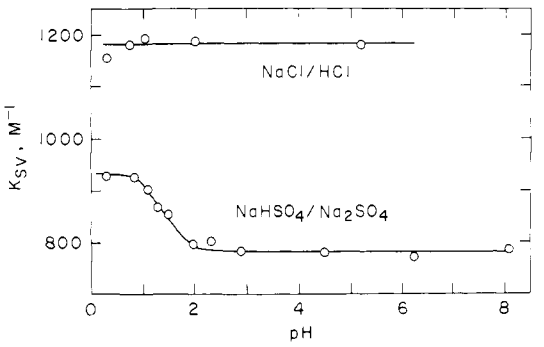

Figure 2. Stern–Volmer constants for quenching of $*Ru(4,4'\text{-}(CH_3)_2bpy)_3^{2+}$ emission by diquat as a function of pH in chloride and sulfate media at 0.5 M ionic strength and 25 °C.

with a Perkin-Elmer Hitachi spectrofluorimeter as a function of quencher Q (bpy, phen, etc.) concentration (excitation wavelength 430–470 nm, emission wavelength 600–630 nm, $[RuL_3^{2+}] = 3 \times 10^{-6}$ M, [Q] = $(0.5\text{–}5) \times 10^{-3}$ M, $\mu = 0.5$ M with NaCl/HCl or $Na_2SO_4/NaHSO_4$). The compositions of the buffered solutions used are given in supplementary Table 1. Quenching rate constants k_q were calculated from $k_q = K_{SV}/\tau_0$ where τ_0 is the excited state lifetime in the absence of added quencher (see ref 10). Flash-photolysis measurements were made as described in ref 10 and pulse-radiolysis experiments as described in ref 14. pH measurements were made with glass combination electrodes on Metrohm or Beckman pH meters; commercial buffers were used in calibrating the electrodes. Absorbances were measured with Cary 17, 210, and 219 spectrophotometers.

Results

pH Dependence of the Emission Quenching. This study was undertaken in order to gain information about the properties of the $bpyH^+$–bpyH· and other LH^+–LH· couples in aqueous solution. Interpretation of the quenching measurements made under a given set of conditions is, however, complicated by the fact that the diprotonated species, e.g., $bpyH_2^{2+}$, are intrinsically better quenchers than the corresponding monoprotonated species and may be responsible for most of the quenching even when LH^+ is the dominant form of L present. This effect is illustrated in Figure 1 where the pH dependence of the quenching of two different sensitizers is contrasted for L = bpy. The pH dependence arises through protonation equilibria and the parallel quenching paths shown in eq 3–7. (The quenching mechanism written is

$$bpyH_2^{2+} \rightleftharpoons bpyH^+ + H^+ \qquad K_{a1} \quad (3)$$

$$bpyH^+ \rightleftharpoons bpy + H^+ \qquad K_{a2} \quad (4)$$

$$*RuL_3^{2+} + bpyH_2^{2+} \rightarrow RuL_3^{3+} + bpyH_2^{+}\cdot \qquad k_a \quad (5)$$

$$*RuL_3^{2+} + bpyH^+ \rightarrow RuL_3^{3+} + bpyH\cdot \qquad k_b \quad (6)$$

$$*RuL_3^{2+} + bpy \rightarrow \qquad k_c \quad (7)$$

justified under Discussion.) For quenching of the $*Ru(4,7\text{-}(CH_3)_2phen)_3^{2+}$ emission (circles) k_b and k_a are comparable, but for $*Ru(5,6\text{-}(CH_3)_2phen)_3^{2+}$ (squares) $k_a \gg k_b$. Even at pH 2.7 where >99% of the total bpy is present as $bpyH^+$ about 20% of the quenching arises through eq 5.

At the onset of this work the quenching measurements were made in sulfate media because the quenchers and sensitizers are both highly soluble in SO_4^-/HSO_4^-. However, because of the need for pH variations below pH 2 the HSO_4^-/SO_4^{2-} equilibrium ($pK_a(HSO_4^-) = \sim 1.33$ at 0.5 M ionic strength, 25 °C[15]) was recognized as a problem: the rate constants for the quenching reactions, which involve the encounter of two cations (eq 5 and 6), are susceptible to specific anion effects. This is illustrated in Figure 2 where the experimental Stern–Volmer constants for quenching of the $*Ru((CH_3)_2bpy)_3^{2+}$ emission by diquat are plotted as a function of pH for both chloride and sulfate media. The chloride values are pH independent, as is expected since

(7) Mulazzani, Q. G.; Emmi, S.; Fuochi, P. G.; Venturi, M.; Hoffman, M. Z.; Simic, M. G. *J. Phys. Chem.* **1979**, *83*, 1582.
(8) Chan, S. F.; Chou, M.; Creutz, C.; Matsubara, T.; Sutin, N. *J. Am. Chem. Soc.* **1981**, *103*, 369.
(9) Krishnan, C. V.; Creutz, C.; Mahajan, D.; Schwarz, H. A.; Sutin, N. *Isr. J. Chem.* **1982**, *22*, 98.
(10) Lin, C-T.; Böttcher, W.; Chou, M.; Creutz, C.; Sutin, N. *J. Am. Chem. Soc.* **1976**, *98*, 6536.
(11) Sutin, N.; Creutz, C. *Adv. Chem. Ser.* **1978**, *No. 168*, 1.
(12) Sutin, N. *J. Photochem.* **1979**, *10*, 19.
(13) Creutz, C.; Keller, A. D.; Sutin, N.; Zipp, A. P. *J. Am. Chem. Soc.* **1982**, *104*, 3618.
(14) Schwarz, H. A.; Creutz, C. *Inorg. Chem.* **1983**, *22*, 707.
(15) Dunsmore, H. S; Nancollas, G. H. *J. Phys. Chem.* **1964**, *68*, 1579.

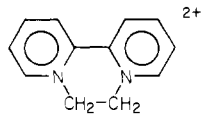

neither diquat nor the sensitizer undergoes protonation in this pH range. By contrast the sulfate/bisulfate data are pH independent above pH ~2 but K_{SV} increases ~15% at low pH. This increase is due to the change of medium from SO_4^{2-} to HSO_4^-. Indeed, the pH dependence of K_{SV} suggests that the pK_a for HSO_4^- is 1.4 ± 0.1, in rather good agreement with the literature value 1.33.[15] In order to simplify the data analysis the pH dependences were carried out in chloride media as well, and Figure 3 contrasts the low pH behavior of some typical sensitizer–quencher combinations.

For data treatment eq 8, which arises from eq 3–7, was used.

$$k_q = \frac{k_a + k_b K_{a1}/[H^+] + k_c K_{a1}K_{a2}/[H^+]^2}{1 + K_{a1}/[H^+] + K_{a1}K_{a2}/[H^+]^2} \qquad (8)$$

With bpy as quencher the best fits were obtained with pK_{a2} = 4.4, which is in good agreement with the recommended value 4.33 ± 0.05.[16] Problems arose, however, with pK_{a1}: reported values range from −0.2 to −0.5[16] while we obtained the best fits (five sensitizers) with pK_{a1} = 0.05. With pK_{a1} = 0.05, 100% bpyH_2^{2+} cannot be produced in the 0.5 M ionic strength media used since the minimum pH obtainable is ~0.3. Thus direct confirmation of the bpy pK_{a1} value proved impossible. The validity of the bpy pK_{a1} value extracted from quenching measurements is, however, supported by results for the dimethylbipyridine system in which pK_{a1} is greater and therefore more readily measured (pK_{a2} = 5.5[16]). For $(CH_3)_2$bpyH_2^{2+} near identical pK_{a1} values were obtained from fits to the quenching data (pK_{a1} = 0.68) and from UV spectral measurements (pK_{a1} = 0.64 ± 0.15; for LH^+ $\epsilon_{288} = 1.20 \times 10^4$ M^{-1} cm^{-1} and $\epsilon_{299} = 1.53 \times 10^4$ M^{-1} cm^{-1}; for LH_2^{2+} $\epsilon_{288} = 1.53 \times 10^4$ M^{-1} cm^{-1} and $\epsilon_{299} = 1.10 \times 10^4$ M^{-1} cm^{-1}). (No literature pK_{a1} value is reported for this amine.)

In fitting the pH dependences, pK_{a2} = 4.4 and pK_{a1} = 0.05 were used for bpy as quencher. The rate constants obtained are summarized in Tables I and II. With Ru(4,7-$(CH_3)_2$phen$)_3^{2+}$, $k_c = 4.3 \times 10^7$ M^{-1} s^{-1}; for the other sensitizers $k_c < 1 \times 10^7$ M^{-1} s^{-1}. Also included in Table II are rate constants for quenching by diquat and by $(CH_3)_2$bpyH_2^{2+} calculated with pK_{a1} = 0.68. Except in the case of Ru(4,7-$(CH_3)_2$phen$)_3^{2+}$ and $(CH_3)_2$bpyH^+ for which $k_b = 1.2 \times 10^8$ M^{-1} s^{-1} (pK_{a2} = 5.5[16]), no quenching by $(CH_3)_2$bpyH^+ or by $(CH_3)_2$bpy was detected (k_b, $k_c \ll 5 \times 10^7$ M^{-1} s^{-1}). Rate constants for quenching by phenH^+ and phenH_2^{2+} calculated with pK_{a2} = 4.9[16] and pK_{a1} = −0.2 (lit.[16] −0.7 to −1.8) are also presented in Tables I and II, respectively. The effect of ionic strength on the diquat quenching rate constant is presented in Figure 4.

Data bearing on the magnitudes of anion effects with diquat, bpyH^+, and bpyH_2^{2+} as quenchers are summarized in Table III. The effects are not especially sensitizer sensitive; for the sensitizers given in Table I the ratio of k_q determined in chloride to that for sulfate varies only from 1.42 to 1.64, with five sensitizers giving 1.50 within experimental error. For Ru(5,6-$(CH_3)_2$phen$)_3^{2+}$, it was verified that the apparent anion dependence of k_q determined from emission intensity measurements was not due to an effect of the anion on the excited-state lifetime; in deaerated water, 0.5 M sodium chloride, and 0.167 M Na_2SO_4 the excited-state lifetimes measured were 1.72, 1.77, and 1.67 μs, respectively—in reasonable agreement with the value (1.81 μs) determined previously in water.[10] This sensitizer was selected because its lifetime is the longest of those used and therefore likely to be the most sensitive to medium effects and because it exhibited the largest k_q discrimination between chloride and sulfate (ratio 1.64).

Flash-photolysis studies of Ru(4,7-$(CH_3)_2$phen$)_3^{2+}$ (2.6×10^{-5} M) and bpy (0.01 M) were made in both 0.4 M H_2SO_4 and 0.125 M $NaHSO_4$/0.125 M Na_2SO_4 at 380, 390, 400, 450, 650, 700, and 750 nm. Neither bpy$H_2^{+\cdot}$ (ϵ_{380} ~3×10^4 M^{-1} cm^{-1} [7]) nor

(16) McBryde, W. A. E. *IUPAC Chem. Data Ser.* **1978**, No. 17.

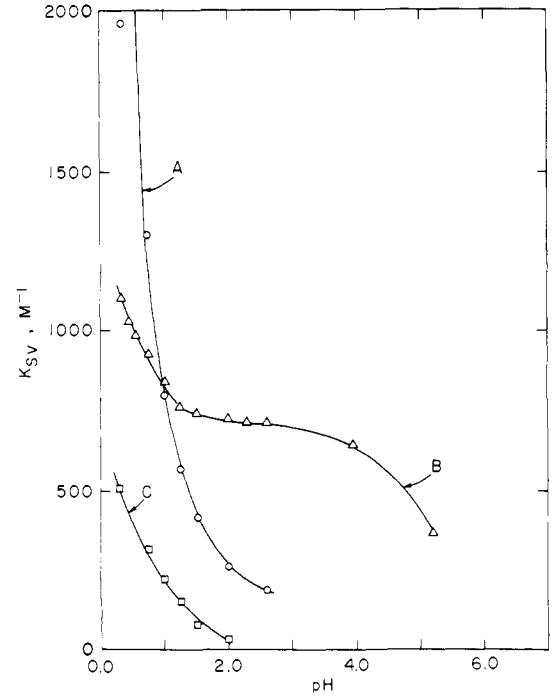

Figure 3. Stern–Volmer constants for quenching of $*RuL_3^{2+}$ emission as a function of pH at 0.5 M ionic strength in chloride media at 25 °C. (A) L = 5,6-$(CH_3)_2$phen, Q = bpy; (B) L = phen, Q = phen; (C) L = bpy, Q = 4,4′-$(CH_3)_2$bpy.

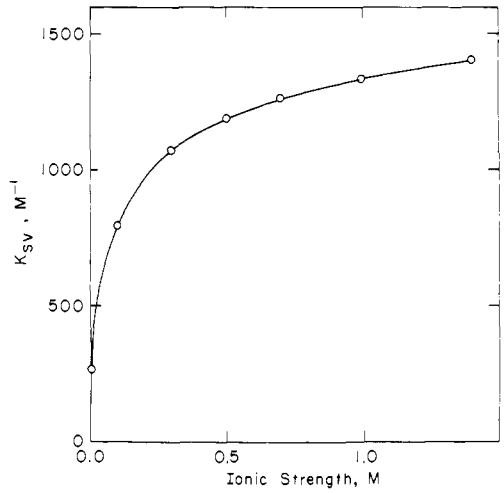

Figure 4. Stern–Volmer constants for quenching of $*Ru(4,4'-(CH_3)_2bpy)_3^{2+}$ emission by diquat as a function of ionic strength (sodium chloride supporting electrolyte, 25 °C).

Table I. Rate Constants for the Quenching of the $*RuL_3^{2+}$ Emission at 25 °C and 0.5 M Ionic Strength in Chloride and Sulfate Media[a]

L	$*E_{3,2}^0$,[b] V	$10^{-9}k_q$, M^{-1} s^{-1}	
		bpyH^+	phenH^+
5-(Cl)phen	−0.77	0.00	0.03 (0.023)
bpy	−0.84	0.00 (0.00)	0.18 (0.13)
phen	−0.87	0.022 (0.01)	0.78 (0.46)
5-(CH_3)phen	−0.90	0.034	1.75
5,6-$(CH_3)_2$phen	−0.93	0.099 (0.06)	
4,4′-$(CH_3)_2$bpy	−0.94	0.61 (0.36)	2.39 (2.06)
4,7-$(CH_3)_2$phen	−1.01	2.44 (1.44)	
3,4,7,8-$(CH_3)_4$phen	−1.11	(3.48)	

[a] Values in parentheses are for sulfate media. [b] Vs. NHE, ref 10.

RuL_3^{3+} was detected following the excited-state decay, with the yield of RuL_3^{3+} and bpy$H_2^{+\cdot}$ produced being <0.05. The low yield of separated redox products is corroborated by continuous pho-

Table II. Rate Constants for the Quenching of the $*RuL_3^{2+}$ Emission at 25 °C in Chloride Media at 0.5 M Ionic Strength[a]

L	$*E_{3,2}°$,[b] V	$10^{-9}k_q$, M^{-1} s^{-1}			
		$bpyH_2^{2+}$	$(CH_3)_2bpyH_2^{2+}$	$phenH_2^{2+}$	$bpy(CH_2)_2^{2+}$
5-(Cl)phen	−0.77	1.70	1.81	0.64	3.06 (1.98)
bpy	−0.84	1.17	1.15 (1.53)	0.92	2.98 (1.96)
phen	−0.87	2.61	2.72	2.83	3.30 (2.32)
5-(CH_3)phen	−0.90	3.16		3.76	3.31 (2.21)
5,6-$(CH_3)_2$phen	−0.93	3.59			3.23 (1.97)
4,4'-$(CH_3)_2$bpy	−0.94	2.58	2.21 (2.91)		3.59 (2.36)
4,7-$(CH_3)_2$phen	−1.01		(2.41)		4.08 (2.76)

[a] Values in parentheses are for sulfate media. [b] Vs. NHE, ref 10.

Table III. Rate Constants for the Quenching of the $*Ru(4,4'-(CH_3)_2bpy)_3^{2+}$ Emission as a Function of Supporting Electrolyte Anion at 0.5 M Ionic Strength[a]

X^-	$10^{-9}k_q$, M^{-1} s^{-1}		
	$bpyH^+$	$bpyH_2^{2+}$ [b]	$bpy(CH_2)_2^{2+}$
F^-			2.42
Cl^-	0.61	1.17	3.59
Br^-	0.85		4.42
I^-			5.84[c]
NO_3^-	0.80	1.54	4.44
SO_4^{2-}	0.36		2.36
HSO_4^-			2.81

[a] Sodium salts were used, 25 °C. [b] The sensitizer is $Ru(bpy)_3^{2+}$. [c] Corrections for the absorbance of the diquat/iodide ion pair were significant.

tolysis results. A solution containing 5.5×10^{-4} M $Ru(bpy)_3^{2+}$, 3×10^{-3} M bpy, 3×10^{-3} M ascorbic acid (to reduce RuL_3^{3+}, if generated) in 1 M H_2SO_4 was irradiated 20 h at $\lambda > 400$ nm, $I_0 = 6 \times 10^{-7}$ einstein s^{-1}: no $bpyH_2$ was detected and less than 0.2 μmol of bpy was lost so that $\phi \leq 1 \times 10^{-5}$ is implicated.

The bipyridine radical protonation equilibrium and equilibration were studied in phosphate buffers by the pulse-radiolysis technique. Deaerated 8×10^{-4} M bpy–2% 2-propanol solutions containing sodium phosphate salts (pH 5–10) were subjected to 0.08-μs pulses of 2-MeV electrons produced by a Van de Graaff accelerator.[14] The OH· formed by water ionization was scavenged by the 2-propanol, giving the 2-propanol radical, while bpy was reduced by the hydrated electron produced in the ionization. The primary product of the reaction, bpy^-·, protonates very rapidly[7] (during the pulse) and the equilibration of the secondary product, bpyH·, with phosphate (eq 9) is observed on the microsecond time scale

$$bpyH· + H_2PO_4^- \underset{k_{-9}}{\overset{k_9}{\rightleftharpoons}} bpyH_2^{+}· + HPO_4^{2-} \qquad (9)$$

in 10^{-3}–10^{-2} M phosphate. (Reduction of bpy by the 2-propanol radical occurs on a much longer time scale under these conditions.) Reaction 9 was followed at 377 nm, where the molar absorptivity of $bpyH_2^{+}$· is much greater than that of bpyH·.[7] The magnitudes of the absorbance changes measured at two phosphate concentrations are plotted as a function of pH in Figure 5A; the line drawn is the calculated curve for the pK_a of $bpyH_2^{+}$· of 7.7 ($pK_a(H_2PO_4^-) = 7.1$). The pseudo-first-order growth of $bpyH_2^{+}$· absorption exhibited a first-order dependence on both $H_2PO_4^-$ and HPO_4^{2-} concentrations, as is expected for the approach to equilibrium eq 9,

$$k_{obsd} = k_9[H_2PO_4^-] + k_{-9}[HPO_4^{2-}]$$

and $K_9 = k_9/k_{-9}$ ($k_{-9} = k_9/4$). The plot shown in Figure 5B permits evaluation of k_9 as 3.2×10^8 M^{-1} s^{-1}.

The above experiments give a value of 7.7 for the pK_a of $bpyH_2^{+}$· at ~0.01–0.05 M ionic strengths and other measurements (vide infra) give $pK_a = 8.2$ at 0.3 M ionic strength. The latter differ somewhat more than would be expected (the value 8.0 is used in subsequent treatments), but both values are substantially greater than reported value 5.6.[7] It is likely that the low value in ref 7 resulted from lack of equilibration; at pH 6 equilibration times may be as long as 10^{-4} s since $[H_3O^+]$ is quite low. In fact, rather high buffer concentrations are required to bring the

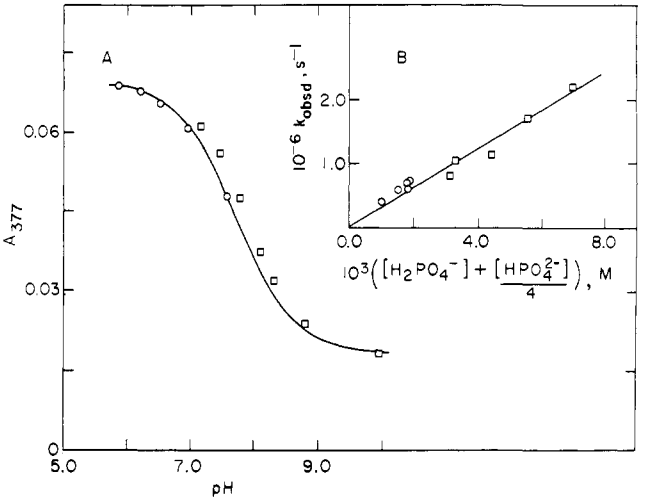

Figure 5. Data for the equilibration $bpyH· + H_2PO_4^- \rightleftharpoons bpyH_2^{+}· + HPO_4^{2-}$. (A) Absorbance at 377 nm as a function of pH at the end of the equilibration; circles, 2×10^{-3} M total phosphate; squares, 1×10^{-2} M total phosphate. (B) Pseudo-first-order rate constant at 377 nm as a function of phosphate concentration.

bpyH·–$bpyH_2^{+}$· equilibration into a convenient time range. By contrast, preliminary experiments with the phenH·–$phenH_2^{+}$· equilibrium, for which the pK_a reported in ref 7 is 6.3, indicate the pK_a to be less than 7—in agreement with the earlier value.[7] Analogous experiments with $(CH_3)_2$bpy yield pK_a ~9.3 for this LH_2^{+}· species at low ionic strength.

In order to evaluate the $E°$ for the LH^+/LH· couples (L = bpy, $(CH_3)_2$bpy) the reactions (eq 10) of LH^+ and LH· with $CoL_3^{+/2+}$,

$$CoL_3^+ + LH^+ \underset{k_{-10}}{\overset{k_{10}}{\rightleftharpoons}} CoL_3^{2+} + LH· \qquad (10)$$

a couple of known $E°$,[9,17] were investigated by the pulse-radiolysis method. For L = bpy, mixtures of Co(II) and bpy in 0.1 M sodium formate (hydroxyl radical scavenger) were studied at 610 nm as a function of $bpyH^+$ and $Co(bpy)_3^{2+}$ concentrations at several pHs. The observations reported here bear only on solutions for which [bpy] > 3 [Co(II)] in which the *tris* complex is the dominant form for both Co(II) and Co(I). Study of the reduction of $Co(bpy)_3^{2+}$ by bpyH· proved straightforward because this reaction proceeds spontaneously above pH ~8. With 2×10^{-3} M bpy and $(0.5–2.0) \times 10^{-4}$ M $Co(bpy)_3^{2+}$, e_{aq}^- reacts quantitatively with bpy (eq 11) to produce bpyH· during the ionizing pulse (k_{11}

$$e_{aq}^- + bpy \rightarrow (bpy^-·) \xrightarrow[-OH^-,\ fast]{H_2O} bpyH· \qquad (11)$$

$= 2.5 \times 10^{10}$ M^{-1} s^{-1} [7]). Production of $Co(bpy)_3^+$ by the reverse of eq 10 is then observed on the microsecond time scale. The top of Figure 6 shows the $Co(bpy)_3^{2+}$ dependence of the Co(I) formation rate constant at pH 9.02 and the insert shows the slopes of such plots obtained at other pHs. The curve drawn through the points is constructed by using $k_{-10} = 4.5 \times 10^9$ M^{-1} s^{-1}, pK_a

(17) Creutz, C.; Krishnan, C. V.; Mahajan, D.; Schwarz, H. A.; Sutin, N., work in progress.

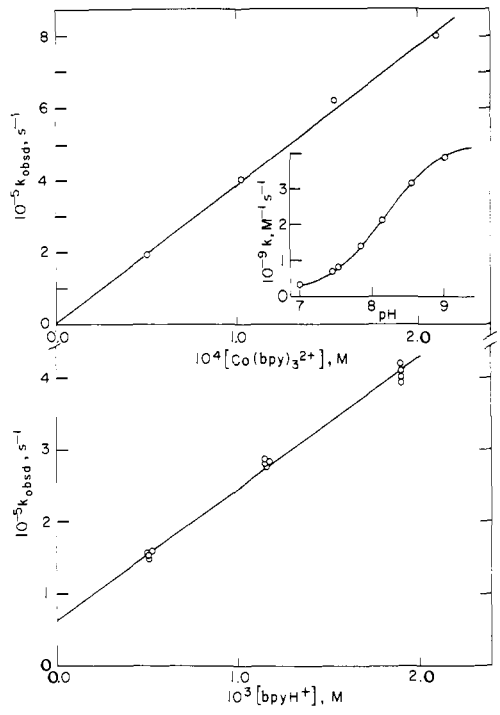

Figure 6. Kinetic data for the equilibration of $Co(bpy)_3^+$ with $bpyH^+$ (eq 10). (Top) Pseudo-first-order rate constants for the reaction of bpyH· with $Co(bpy)_3^{2+}$ as a function of the concentration of $Co(bpy)_3^{2+}$ at pH 9.02. The insert shows the pH-dependence of the slopes of such plots determined at other pHs. (Bottom) Pseudo-first-order rate constants for reaction of $Co(bpy)_3^+$ with $bpyH^+$ as a function of $bpyH^+$ concentration determined at pH 4.

= 8.2 for $bpyH_2^{+}$· at ~0.3 M ionic strength, and assumes that $bpyH_2^{+}$· does not reduce $Co(bpy)_3^{2+}$ ($k \leq 1 \times 10^8$ M^{-1} s^{-1}). Since eq 10 is unfavorable as written, in order to directly measure k_{10} it was necessary to rapidly drive the reaction to the right through rapid protonation of bpyH·. Because of the rapidity of the reverse reaction, high buffer concentrations were required. The determination of k_{10} proved feasible in 0.1 M formate, 0.1 M acetate solutions at pH 4.01 with $[Co(bpy)_3^{2+}] = 2.8 \times 10^{-3}$ M and $[bpyH^+] = (0.5\text{–}2) \times 10^{-3}$ M. Production of $Co(bpy)_3^+$ occurred during the pulse through eq 12 ($k_{12} = 7.7 \times 10^{10}$ M^{-1} s^{-1} [9]) and

$$e_{aq}^- + Co(bpy)_3^{2+} \rightarrow Co(bpy)_3^+ \qquad (12)$$

was followed by a small absorbance increase due, to a small extent, to formate–radical reduction of Co(II) ($k = 5 \times 10^7$ M^{-1} s^{-1}); the bulk of the formate radical decay occurs through

$$\cdot CO_2^- + bpyH^+ \rightarrow CO_2 + bpyH\cdot$$

($k = 5 \times 10^8$ M^{-1} s^{-1} [7]), which is also seen at 610 nm. Subsequently, the spectrum of $Co(bpy)_3^+$ was transformed to that of $bpyH_2^{+}$·.[7,9] Pseudo-first-order rate constants for this change (determined at 610 nm) are plotted vs. $[bpyH^+]$ at the bottom of Figure 6. The slope of the line drawn there is $k_{10} = 1.84 \times 10^8$ M^{-1} s^{-1} (at ~0.25 M ionic strength). The intercept is attributed to a small constant error in $[bpyH^+]$ which corresponds to a 3% error in the ratio of the total bpy to total Co(II) concentrations. From the ratio of the forward and reverse rate constants $K_{10} = (4.1 \pm 0.2) \times 10^{-2}$ is obtained.

The measurement of the rate and equilibrium constants for eq 10 with L = $(CH_3)_2bpy$ was analogous to that described above for the bpy system, but the experimental conditions used were somewhat different. Experiments at pH 4.4, as presented in Figure 6 for bpy, gave $k_{10}((CH_3)_2bpy) = 4.3 \times 10^8$ M^{-1} s^{-1} under the following conditions: 0.13 M 2-propanol, 0.03 M acetic acid, 1.0 $\times 10^{-3}$ M $CoSO_4$, (3–4) $\times 10^{-3}$ M total $(CH_3)_2bpy$. (2-Propanol was used as OH-scavenger instead of formate because reaction of 2-propanol radical with $(CH_3)_2bpyH^+$, $k \leq 5 \times 10^7$ M^{-1} s^{-1}, is so slow that it takes place after reaction 10, simplifying the observation of the latter.) The magnitude of $k_{-10}((CH_3)_2bpy) =$ 3.3×10^9 M^{-1} s^{-1} was measured at pH 10.2 (no added buffer) in the presence of 1.0×10^{-4} M $CoSO_4$, 5.8×10^{-4} M total $(CH_3)_2bpy$, and 0.2 M methanol. No correction for the ~10% $(CH_3)_2bpyH_2^{+}$· present at equilibrium was made because this equilibration was too slow to be of account in the absence of added buffer. The ratio k_{10}/k_{-10} gives $K_{10} = 0.13 \pm 0.01$ for $(CH_3)_2bpy$.

Scheme I

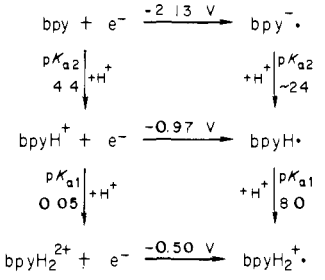

Scheme II

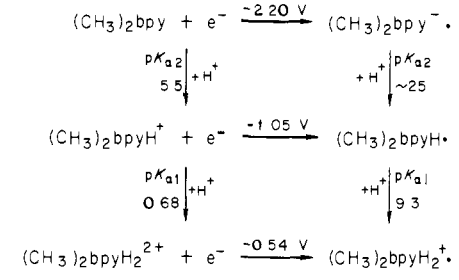

Discussion

The pulse-radiolysis studies of the CoL_3^{+}–LH^+ equilibration permitted evaluation of K_{10} as 4.1×10^{-2} and 1.3×10^{-1} for bpy and $(CH_3)_2bpy$, respectively. From these values of K_{10}, the reduction potential of the $Co(bpy)_3^{2+/+}$ couple (–0.89 V[9]), and the reduction potential of the $Co((CH_3)_2bpy)_3^{2+/+}$ couple (–1.00 V[9]), the reduction potentials for the $bpyH^+$–bpyH· and $(CH_3)_2bpyH^+$–$(CH_3)_2bpyH$· couples are calculated to be –0.97 and –1.05 V, respectively. (All $E°$'s given vs. NHE.) From the difference in the pK_a values for LH_2^{2+} and LH_2^{+}· and the above LH^+–LH· $E°$'s the reduction potentials for the LH_2^{2+}–LH_2^{+}· couples are obtained, and the pK_a of LH· is estimated from the difference in $L\text{–}L^{-}$·[1,18] and LH^+–LH· potentials. These thermodynamic parameters are summarized in Schemes I and II for bpy and $(CH_3)_2bpy$, respectively. In addition the high pH experiments of Erhard and Jaenicke[3–5] implicate[19] the reduction potential for eq 13 to be –0.64 V from which (using pK_{a1} and pK_{a2} for bpy)

$$bpy + 2H^+ + 2e^- = bpyH_2 \qquad (13)$$

the $E°$ for reaction 14 is –0.51 V. From this potential and the

$$bpyH_2^{2+} + 2e^- = bpyH_2 \qquad (14)$$

$bpyH_2^{2+}$–$bpyH_2^{+}$· reduction potential, the potential –0.52 V for the $bpyH_2^{+}$·–$bpyH_2$ couple is estimated.

The pK_a and $E°$ values summarized in Scheme I are of value in interpreting the quenching of $*RuL_3^{2+}$ by bpy and its protonated forms. Three general quenching mechanisms, eq 15–17, are

$$*RuL_3^{2+} + Q \rightarrow RuL_3^{+} + Q^+ \qquad (15)$$

$$*RuL_3^{2+} + Q \rightarrow RuL_3^{2+} + *Q \qquad (16)$$

$$*RuL_3^{2+} + Q \rightarrow RuL_3^{3+} + Q^- \qquad (17)$$

encountered. Reductive quenching, eq 15, is expected to be inefficient for bpy (and also for phen and $(CH_3)_2bpy$) because of the high values of the bpy^{+}·–bpy, etc., potentials. No oxidation of bpy or phen is observed in acetonitrile ($E°$ for $L\text{–}L^{+}$· > ~2 V),[1] and the protonated species are presumably even more difficult

(18) Elliott, C. M.; Hersenhart, E. J. *J. Am. Chem. Soc.* **1982**, *104*, 7519.
(19) Creutz, C. *Comments Inorg. Chem.* **1982**, *1*, 293.

Scheme III

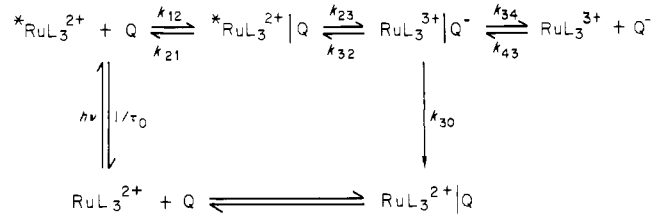

to oxidize; the bpy–bpy$^{+\cdot}$ potential when bpy is bound to +3 metal centers is ~+2.8 V.[20] Since the $*RuL_3^{2+}$–RuL_3^{+} reduction potentials relevant to eq 15 range only up to ~+1 V,[11] it is apparent that eq 15 is likely to be unfavorable by ≥1 eV for the systems studied here. In addition, energy-transfer quenching, eq 16, is expected to be slow because of the high excited-state energies of the aromatic amines.[21] By contrast, oxidative quenching, eq 17, is thermodynamically feasible for many of the sensitizer–quencher pairs studied. The RuL_3^{3+}–$*RuL_3^{2+}$ reduction potentials range from −0.77 to −1.1 V and are listed as a function of L in Tables I and II. Thus quenching by $bpyH_2^{2+}$ should proceed spontaneously for all of the sensitizers used. In accord with this, close to diffusion-controlled rate constants are found with Q = $bpyH_2^{2+}$ and the other dipositive quenchers in Table II. Quenching by bpy ($E°$ = −2.1 V) is not expected by this or any other mechanism and is not observed. Since the reduction potential of $bpyH^+$ (−0.97 V) is intermediate in value, reaction should be rapid with some, but not all, of the sensitizers. This prediction is borne out in the rate constants for $bpyH^+$ quenching listed in Table I. The k_q values range from less than 10^7 M^{-1} s^{-1} for the poor reducing agents (top of table) to greater than 10^9 M^{-1} s^{-1} for the strongest reducing agents.

Since either endergonic ($*E°_{3,2} \leq -0.97$ V) or exergonic electron transfer may occur depending upon the nature of $*RuL_3^{2+}$, the detailed model for oxidative quenching given in Scheme III will be used to treat the $bpyH^+$ quenching data. Scheme III leads to eq 18 for k_{qc}, the diffusion-corrected quenching rate constant ($1/k_q = 1/k_{qc} + 1/k_{diff}$).

$$k_{qc} = \frac{K_{12}k_{23}}{1 + k_{32}/(k_{30} + k_{34})} \tag{18}$$

In order to treat the free-energy dependence of the quenching rate constants [13,21] we use eq 19

$$k_{qc} = \frac{K_{12}\nu_{23}\kappa_{23}\exp(-\Delta G_{23}^*/RT)}{1 + \nu_{23}\kappa_{23}\exp((\Delta G_{23}° - \Delta G_{23}^*)/RT)/(k_{30} + k_{34})} \tag{19}$$

where

$$K_{12} = \frac{4\pi N r^2 \delta r}{1000}\exp(-w/RT)$$

$$k_{23} = \nu_{23}\kappa_{23}\exp(-\Delta G_{23}^*/RT)$$

$$\Delta G_{23}^* = \frac{\lambda_{23}}{4}\left[1 + \frac{\Delta G_{23}°}{\lambda_{23}}\right]^2$$

In the above equations r is the separation of the centers of the two reactants in the precursor complex, δr is the thickness of the reaction layer (~0.8 Å), w is the work required to bring the two reactants together, ν_{23} is a nuclear frequency factor, and κ_{23} is the electronic factor for the reactions (in the normal free energy region κ = 1 for an adiabatic reaction; $\kappa \ll 1$ for a nonadiabatic reaction). The reorganization parameter for the quenching reaction, λ_{23}, is related to the reorganization parameters λ_{22} and λ_{33} for the two couples involved by

$$\lambda_{23} = \frac{\lambda_{22} + \lambda_{33}}{2} \tag{20}$$

(20) Gaudiello, J. G.; Sharp, P. R.; Bard, A. J. *J. Am. Chem. Soc.* **1982**, *104*, 6373.

(21) Bock, C. R.; Connor, J. A.; Gutierrez, A. R.; Meyer, T. J.; Whitten, D. G.; Sullivan, B. P.; Nagle, J. K. *J. Am. Chem. Soc.* **1979**, *101*, 4815.

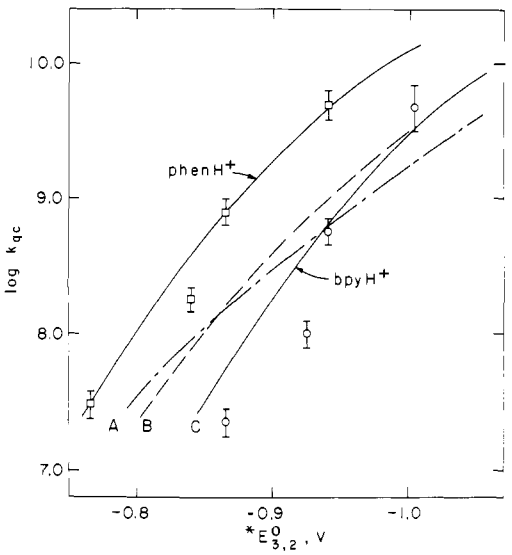

Figure 7. Logarithm of k_{qc}, the diffusion-corrected rate constant for quenching of $*RuL_3^{2+}$ emission, as a function of the $*RuL_3^{2+}$ reduction potential for $bpyH^+$, circles, and $phenH^+$, squares, as quenchers. The calculated curves are explained in the text.

The expression for k_{qc} (eq 19) contains the parameters K_{12}, λ_{23}, K_A, $\nu_{23}\kappa_{23}$, and $(k_{30} + k_{34})$, in addition to the driving force which is obtained from $E°$ differences. The preequilibrium constant K_{12} is estimated to be 0.3 M^{-1} for reactants of these sizes at 0.5 M ionic strength. From the large values of the rate constants for eq 10, for which the driving force is only 0.08 eV, it is evident the self-exchange rate for the $bpyH^+$–bpyH$\cdot$ couple must be very large ($\geq 1 \times 10^9$ M^{-1} s^{-1}); the RuL_3^{3+}–$*RuL_3^{2+}$ self-exchange rates are also known to be quite high.[10-12] Thus the intrinsic kinetic barrier λ_{23} must be quite small, and we have used trial values only in the range 0.08–0.23 eV. The values of ν_{23} depends upon the relative magnitudes of the inner-sphere ($\nu_{in} \simeq 10^{13}$ s^{-1}) and solvent ($\nu_{out} \simeq 10^{12}$ s^{-1}) barriers,[22] and values of ν_{23} ranging between 10^{12} and 10^{13} s^{-1} were tried. The values of $(k_{30} + k_{34})$ used ranged from 10^{12} s^{-1} to 5×10^{10} s^{-1} (implicated from studies of related bipyridine systems[13]). In all calculations k_{diff} was taken as 5×10^9 M^{-1} s^{-1}, work term corrections to the driving force were neglected, and κ was taken as 1.

The data for quenching by $bpyH^+$ (and $phenH^+$; vide infra) are plotted in Figure 7 as a function of $E°$ for the $*RuL_3^{2+}$–RuL_3^{3+} couples. The curves shown correspond to different combinations of the parameters in eq 19. Curves A and B illustrate the effects of changing λ_{23} and $\Delta G_{23}°$ at constant $\nu_{23} = 10^{13}$ s^{-1} and $(k_{30} + k_{34}) = 10^{12}$ s^{-1}. Curve B corresponds to $E°$($bpyH^+$–bpyH$\cdot$) = −0.97 V and $k_{11}k_{22} = 10^{19}$ M^{-2} s^{-2} (λ_{23} = 0.18 eV). In order to obtain a comparable fit (curve A) with the smaller self-exchange rate product 10^{17} M^{-2} s^{-2} (λ_{23} = 0.23 V) smaller $\Delta G_{23}°$ values are required and curve A corresponds to $E°$($bpyH^+$–bpyH$\cdot$) = −0.87 V, considerably more positive than the value obtained from our studies of reaction 10. For curve C, fit B was taken as the point of departure and the magnitude of $(k_{30} + k_{34})$ was reduced to 5×10^{10} s^{-1} in an effort to better fit the left-hand points (circles). The improvement in the fit to the data is apparent. As mentioned earlier, for dipositive organic bpy derivatives such as diquat k_{30} values in the range (2–4) $\times 10^{10}$ s^{-1} were estimated from cage-escape yields, which were of the order of 0.2. No cage escape ($\Phi < 0.05$) was detected in the $bpyH^+$–$*RuL_3^{2+}$ reactions, suggesting a larger k_{30}/k_{34} ratio for these systems. Probably the lowered cage-escape yields in the $bpyH^+$ (and $bpyH_2^{2+}$) systems result from the combined effects of slightly larger k_{30} and slightly smaller k_{34} values.

Also shown in Figure 7 is the free-energy dependence of quenching by $phenH^+$. These data present a different problem because $E°$ for the $phenH^+$–phenH$\cdot$ couple is unknown. By

(22) Sutin, N. *Acc. Chem. Res.* **1982**, *15*, 275.

Scheme IV

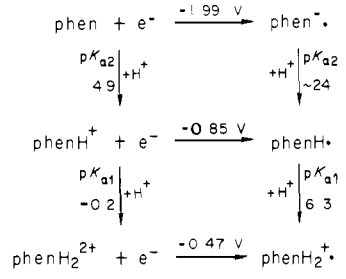

Table IV. Reduction Potentials for 2,2'-Bipyridine, 4,4'-Dimethyl-2,2'-bipyridine, 1,10-Phenanthroline, and Their N-Substituted Derivatives

	bpy		$(CH_3)_2$phen		phen	
couple	E°, V	ref	E°, V	ref	E°, V	ref
$L^{0/-}$	−2.13	1	−2.20	18	−1.99	22
$LH^{+/0}$	−0.97	*a*	−1.05	*a*	−0.85	*a*
$LH_2^{2+/+}$	−0.50	*a*	−0.54	*a*	−0.47	*a*
$L(CH_2\text{-})_2^{2+/+}$	−0.38	13	−0.48	18		
$L(CH_3)_2^{2+/+}$	−0.73	24				
$CrL_3^{0/-}$	−1.89	18				
$FeL_3^{2+/+}$	−1.26	23	−1.34	23	−1.39	22
$RuL_3^{2+/+}$	−1.33	1	−1.34	23	−1.41	1
$[RuL_3^{3+/2+*}]^b$	−0.84	10	−0.94	10	−0.87	10
$IrL_3^{3+/2+}$	−0.83	26			−0.94	26

[a] Value obtained in this work. [b] The RuL_3^{3+}-$*RuL_3^{2+}$ couple.

drawing on the $bpyH^+$ fits, however, this E° can be estimated. If it is assumed that the $phenH^+$ and $bpyH^+$ systems are similar in their intrinsic parameters (K_{12}, ν_{23} κ_{23}, λ_{23}, and $(k_{30} + k_{34})$), but differ in E°, fit C for bpy, displaced along the horizontal axis, should also provide a good fit of the $phenH^+$ quenching rate constants. In fact, the solid curve drawn through the $phenH^+$ points (squares) in Figure 7 is the bpy curve C displaced by 0.12 V, and it is evident that this curve does indeed provide an excellent fit of the phen data. Since the bpy curve has been shifted 0.12 V, the $phenH^+$–phenH· reduction potential is estimated as −0.85 ± 0.05 V.

Although E° for the $phenH^+$–phenH· couple is on somewhat less firm ground than the corresponding value for the bpy and $(CH_3)_2$ bpy systems, it is worthwhile to summarize the thermodynamic parameters for phen as was done in Schemes I and II. This is done in Scheme IV in which the E° for the phen–$phen^-$· couple is taken from the literature,[23] as is the pK_a of $phenH_2^{+}$·;[7] the pK_a values for $phenH_2^{2+}$ and $phenH^+$ were established in this study and the $phenH^+$–phenH· E° was estimated above. The remaining values in Scheme IV were calculated from combinations of the other parameters as was detailed for bpy and $(CH_3)_2$bpy.

Reduction potentials for bpy and phen derivatives have been extensively studied[1,23-26] and discussed.[18,19,24a,25] In Table IV data for bpy and phen based species are compared. As has been noted by others: (a) differences in the reducibility of the uncomplexed aromatic amines L tend to persist in complexed derivatives such as ML_3^{2+} or $L(CH_2\text{-})_2^{2+}$; that is, bpy derivatives are generally more readily reduced than $(CH_3)_2$bpy derivatives. In a number of related systems extensive correlation of L-derivative reduction potential with L-potential have been recorded.[18,24,25] (b) The largest changes in E° are, however, produced by changing the charge on L.[19827] For the species given in Table IV the reduction potentials range over more than 1.5 V when positively charged centers (H^+, etc.) are attached to the nitrogen atoms of L.

Table IV also presents a convenient summary of the answers to the questions that originally motivated this work. In the RuL_3^{2+} photoconversion systems both $*RuL_3^{2+}$ and RuL_3^{+} are used as intermediary reductants in the presence of LH^+ and LH_2^{2+}. The relatively high E° values of the LH_2^{2+}–LH_2^{+}· couples assure that LH_2^{2+} will oxidize RuL_3^{+} and most $*RuL_3^{2+}$ species regardless of the L combination chosen. Oxidation of RuL_3^{+} by LH^+ is also generally favored, but the oxidation of $*RuL_3^{2+}$ by LH^+ depends strongly on the L combination chosen. Interestingly, however, since no separated products result from the LH^+/LH_2^{2+}–$*RuL_3^{2+}$ reactions, these reactions result only in excited-state quenching and lowered overall efficiencies; by contrast, the LH_2^{2+}–RuL_3^{+} and LH^+–RuL_3^{+} reactions may result in net reduction of L to LH_2, etc.[9]

Finally, some comment on the electron-exchange rate constants for the various couples studied here is appropriate. The analyses for $bpyH^+$ and $phenH^+$ quenching presented above yield estimated self-exchange rates for the LH^+–LH· couples of $\geq 10^9$ M^{-1} s^{-1}. The use of such large values is also required by the high rate constants for eq 10, the CoL_3^{+}–LH^+ equilibration. Relatively large exchange rates for related metal-bound L–L^-· couples have previously been implicated[18] in electrochemical[2,24,26] and photochemical work.[11,12] Our kinetic data for the CoL_3^{+}–LH^+ systems (eq 10) also require large values for the CoL_3^{2+}–CoL_3^{+} electron exchanges. By contrast, the LH_2^{2+}–LH_2^{+}· exchanges appear (from the data given in Table II) to be substantially slower: For example, with an estimate of $k_{diff} = 4 \times 10^9$ M^{-1} s^{-1} for the $*RuL_3^{2+}$/$bpyH_2^{2+}$ reactions the activation-controlled rate constant for L = 5-(Cl) phen (0.27 V driving force) is 3.0×10^9 M^{-1} s^{-1}. A crude application of the Marcus cross-relation[13,28] using 1×10^9 M^{-1} s^{-1} as the $*RuL_3^{2+}$–RuL_3^{3+} exchange rate suggests that the $bpyH_2^{2+}$–$bpyH_2^{+}$· exchange rate is $\sim 10^5$ M^{-1} s^{-1}, quite similar to values implicated previously[13] for the dipositive alkyl N-substituted derivatives (diquat, etc.). This small but surprising reactivity difference is not, at present, understood.[29]

Conclusions

A combination of pulse-radiolysis and emission quenching techniques has been used to establish the redox characteristics of several aromatic amine–amine radical couples. Protonation of these amines favors their reduction to the corresponding radicals by more than a volt for the singly protonated amines and by about an additional 0.5 V for the diprotonated amines. All the aromatic amine–radical couples exhibit small outer-sphere electron-transfer barriers (rapid self-exchange rates).

Acknowledgment. This work was performed at Brookhaven National Laboratory under the auspices of the U. S. Department of Energy and supported by its Office of Basic Energy Sciences.

Supplementary Material Available: The compositions of solutions used for pH dependence studies in 0.5 M ionic strength sulfate media (1 page). Ordering information is given on any current masthead page.

(23) Musumeci, S.; Rizzarelli, E.; Fragala, I.; Sammartano, S.; Bonomo, R. P. *Inorg. Chim. Acta* **1973**, *7*, 660.
(24) (a) Saji, T.; Aoyagui, S. *J. Electroanal. Chem.* **1975**, *63*, 31. (b) *Ibid.* **1975**, *58*, 401 and references cited therein.
(25) Vlcek, A. A. *Coord. Chem. Rev.* **1982**, *21*, 99 and references cited therein.
(26) (a) Kew, G.; Hanck, K.; DeArmond, K. *J. Phys. Chem.* **1974**, *78*, 727. (b) *Ibid.* **1975**, *79*, 1828. (c) Kahl, J. L.; Hanck, K. W.; DeArmond, K. *J. Phys. Chem.* **1978**, *82*, 540. (d) *Ibid.* **1979**, *83*, 2611.
(27) Noteworthy exceptions to this rule (which *does* hold for a wide variety of methyl-substituted species) are the 4- and 5-substituted $-COOC_2H_5$ derivatives of bpy which are 0.5–0.8 V more readily reduced than bpy.[18]
(28) Marcus, R. A. *Annu. Rev. Phys. Chem.* **1964**, *15*, 155.
(29) Although the reactivity differences are real, it should be noted that the exchange rates are derived using a model formulated for spherical reactants.